Statistical subspace-based damage detection with estimated reference

Eva Viefhues, Michael Döhler, Falk Hille, Laurent Mevel

Statistical subspace-based damage detection with estimated reference[☆]

Eva Viefhues[a,b,*], Michael Döhler[b], Falk Hille[a], Laurent Mevel[b]

[a] *BAM Federal Institute for Materials Research and Testing, Division 7.2 Buildings and Structures, Unter den Eichen 87, 12205 Berlin, Germany*
[b] *Univ. Gustave Eiffel, Inria, COSYS/SII, I4S, Campus de Beaulieu, 35042 Rennes, France*

Abstract

The statistical subspace-based damage detection technique has shown promising theoretical and practical results for vibration-based structural health monitoring. It evaluates a subspace-based residual function with efficient hypothesis testing tools, and has the ability of detecting small changes in chosen system parameters. In the residual function, a Hankel matrix of output covariances estimated from test data is confronted to its left null space associated to a reference model. The hypothesis test takes into account the covariance of the residual for decision making. Ideally, the reference model is assumed to be perfectly known without any uncertainty, which is not a realistic assumption. In practice, the left null space is usually estimated from a reference data set to avoid model errors in the residual computation. Then, the associated uncertainties may be non-negligible, in particular when the available reference data is of limited length. In this paper, it is investigated how the statistical distribution of the residual is affected when the reference null space is estimated. The asymptotic residual distribution is derived, where its refined covariance term considers also the uncertainty related to the reference null space estimate. The associated damage detection test closes a theoretical gap for real-world applications and leads to increased robustness of the method in practice. The importance of including the estimation uncertainty of the reference null space is shown in a numerical study and on experimental data of a progressively damaged steel frame.

Keywords: Damage detection, Uncertainty quantification, Statistical tests, Ambient excitation, Vibration measurement

1. Introduction

Vibration-based structural health monitoring (SHM) of civil or mechanical structures is based on the fact that the dynamical behavior of a structure is affected by damage [1]. The detection of damage is a fundamental task for SHM, before further levels of damage diagnosis concerning damage localization,

[☆] A preliminary version of this paper was presented at the 10th IFAC Symposium on Fault Detection, Diagnosis and Safety of Technical Processes (SAFEPROCESS), August 29 – 31, 2018, Warsaw, Poland.

[*] Corresponding author; *E-mail address: eva.viefhues@bam.de*

quantification and lifetime prediction can be reached [2]. The basic premise is that damage will alter the stiffness, mass or damping properties of the structure, and consequently its dynamic properties, so it can be inferred based on the measured vibration response of the system. Output-only methods based on the assumption of ambient excitation are particularly interesting in this context, as dynamic properties can be evaluated under normal operating conditions and without human interaction. Damage detection can then be accomplished purely data-driven by evaluating changes in damage-sensitive features that are extracted from the measurements in a (healthy) reference state of the system and the current test state [3]. Since the features are computed from ambient vibration data, they are subject to statistical variability. Hence, the statistical properties of the feature need to be considered properly for its evaluation in order to decide if a change is significant, i.e. if there is damage or not. This paper investigates damage detection under statistical uncertainty related to both reference and test states in the context of subspace-based damage detection [4, 5].

There are many ways to define and evaluate features for damage detection. Reviews of vibration-based damage detection methods can be found in [6–8]. Damage features are e.g. based on modal parameters [9–11], parameters of (combined) auto-regressive models [12, 13], Kalman filter innovations [14, 15], wavelet transform [16], neural networks [17], and many other features from signal processing [18, 19]. Feature evaluation methods often rely on an outlier or novelty analysis [20, 21], investigating the statistical properties of the damage feature. They are based on the Mahalanobis distance [22], whiteness tests [14], clustering methods [23], statistical process control [24], and other statistical hypothesis tests. Based on the distribution properties of the feature and an allowed false positive error probability, a threshold for the decision between healthy or damaged can e.g. be determined empirically from several reference data sets in the healthy state. Similarly, control charts known from statistical process control are widely applied in vibration-based SHM e.g. [13, 15, 24, 25], mainly but not exclusively focusing on uni-variate control charts such as X-Bar charts to monitor the statistical properties of scalar features. In many works it is highlighted that the proper consideration of uncertainties of the damage sensitive feature is of crucial importance to avoid false alarms and to guarantee a reliable damage detection procedure. Several approaches therefore aim for automated uncertainty consideration in damage detection methods, e.g. by means of genetic algorithms [26], fuzzy logic approaches [27], or – in the field of model-updating procedures – Bayesian methods [28] and approaches using interval arithmetic [29]. Other approaches focus on explicit uncertainty quantification models of damage sensitive features such as Frequency Response Functions and modal parameters [30, 31]. In this context, the statistical subspace-based damage detection (SSDD) method [4, 5, 32] has the advantage of characterizing precisely the statistical behavior of the damage detection tests for both healthy and damage scenarios, affected by the uncertainties of the tested data resulting from measurement and excitation noise. Being based on a powerful statistical framework for parametric change detection [33], the method has been extended with robustness to changing ambient excitation [5, 34] and temperature conditions [35–37].

Moreover, damage localization and quantification are possible with the considered feature in connection with finite element model-based sensitivities in the same framework [32, 38, 39]. Successful applications on field data have been reported e.g. in [40, 41]. The objective of this paper is to address the robustness of the method towards uncertainties related to the estimation of the reference for the damage feature.

In the SSDD method, the feature is a subspace-based residual vector, which is based on subspace properties of the Hankel matrix of output covariances. It is defined as the product of the left Hankel matrix null space of the reference state and the Hankel matrix computed on current measurement data in the test state [4, 5]. The statistical evaluation of the residual in an associated hypothesis test yields a damage detection test statistic that considers the uncertainty related to the test data. The test is straightforward to compute from the data, without the need of modal parameter estimation and tracking in the test state, nor other complex numerical operations. While the previously cited works show a wide applicability of the subspace-based residual for damage diagnosis, only the uncertainty related to the Hankel matrix estimate of the test data is currently taken into account in its statistical evaluation, implicitly assuming that the left null space computed in the reference state is free of uncertainty. This is only adequate for the theoretical case where the reference null space is computed from a (perfect) model [4], which is not realistic in practice where the null space is usually estimated from a reference data set [35, 40]. Then, the associated uncertainties may be non-negligible, in particular when the available reference data is of limited length. In this paper, the impact of the reference null space uncertainty on the statistical distribution of the residual is analyzed. Based on the obtained distribution properties, a damage detection test is developed that takes into account the uncertainties related to measurements of both the reference state (for the residual setup) and to the current state (for the residual evaluation), while the former has not been considered in previous works. Since in practice the reference state is never perfectly known, the developed test closes a theoretical gap for real-world applications and leads to increased robustness of the method. The resulting test performance is evaluated with a numerical example and demonstrated on experimental data.

This paper is organized as follows. In Section 2, the background of the damage detection approach is recalled. In Section 3, the asymptotic distribution of the subspace-based residual is analyzed under estimation uncertainties in the reference, and the respective test statistic is developed for damage detection. Finally, the method is validated on a numerical example given in Section 4, and applied to experimental data of a progressively damaged steel frame in Section 5.

2. Background and problem statement

2.1. Damage detection methodology

It is assumed that the vibration behavior of the investigated structure can be described by a linear time-invariant dynamical system, with corresponding discrete-time stochastic state space system [42]

$$\begin{cases} x_{k+1} = Ax_k + w_k \\ y_k = Cx_k + v_k, \end{cases} \tag{1}$$

where $A \in \mathbb{R}^{n\times n}$ is the state transition matrix, $C \in \mathbb{R}^{r\times n}$ is the observation matrix, $x_k \in \mathbb{R}^n$ is the state vector, $y_k \in \mathbb{R}^r$ contains the measured outputs at r sensor positions at discrete time index k, n is the model order, and $w_k \in \mathbb{R}^n$ and $v_k \in \mathbb{R}^r$ are the state noise and output noise, respectively, which are unmeasured, and assumed to be white, stationary, centered and having finite fourth moments.

The subspace-based damage-sensitive feature vector [4, 5] has been developed based on properties of the output-only covariance-driven subspace method [43], where an estimate of the block Hankel matrix $\mathcal{H}$ containing the output covariances of the monitored system is computed. Due to the well-known factorization property of this matrix into observability and controllability matrix [43, 44], its image *subspace* contains the dynamic characteristics of the structure and is thus sensitive to damages. Thanks to this property, the subspace-based feature or *residual vector* is defined based on the left null space S_0 of the theoretical Hankel matrix $\mathcal{H}^{(0)}$ in the reference state and the Hankel matrix estimate $\widehat{\mathcal{H}}$ computed on a data set of length N in the current test state as

$$\zeta = \sqrt{N}\,\mathrm{vec}(S_0^T\widehat{\mathcal{H}}), \tag{2}$$

where $\mathrm{vec}(\cdot)$ is the column stacking vectorization operator. Hence, its mean is zero when the system is in the reference state and deviates from zero when the system is damaged. It should be noted that this property does not only hold for the block Hankel matrix associated to the covariance-driven subspace method. In fact, it is a general property of the family of subspace methods, where a matrix $\widehat{\mathcal{H}}$ is computed from the measurements with different kinds of projections such that the image subspace of this matrix is the observability matrix [44, 45].

Since the residual is computed from data, it is subject to uncertainties that have to be taken into account for a decision if the deviation from zero is significant, i.e. if there is damage. For this, the system state is first formalized by a parameter vector θ that characterizes the system. For example, it is a vector containing the modal parameters or damage-sensitive structural design parameters. Its value in the reference state is θ_0. Based on the computed residual ζ in (2), a decision is made during monitoring between the hypotheses

$$\begin{aligned} &\mathbf{H}_0 :\ \theta = \theta_0 && \text{(reference system)}, \\ &\mathbf{H}_1 :\ \theta = \theta_0 + \delta/\sqrt{N} && \text{(damaged system)}, \end{aligned} \tag{3}$$

where δ is an unknown but fixed change vector. Note that the alternate hypothesis $\mathbf{H}_1$ corresponds to a formulation of "$\theta \neq \theta_0$" for the analysis with the local asymptotic approach to change detection [33], which allows the characterization of the residual distribution in the damaged state. This framework has the advantage of being able to characterize small changes in the system if the data length N of the test data is large enough. In this setting, it has been shown that the residual is approximately Gaussian distributed, satisfying

$$\zeta \xrightarrow{d} \begin{cases} \mathcal{N}(0, \Sigma) & \text{under } \mathbf{H}_0 \\ \mathcal{N}(\mathcal{J}\,\delta, \Sigma) & \text{under } \mathbf{H}_1 \end{cases} \tag{4}$$

for $N \to \infty$, where $\mathcal{J}$ is the asymptotic sensitivity with respect to parameter θ (evaluated at θ_0), Σ is the covariance of the residual, and "d" denotes convergence in distribution. It is assumed that $\mathcal{J}$ has full column rank and Σ is positive definite. Following (4), the damage detection problem corresponds to detecting changes in the mean of a Gaussian variable. The generalized likelihood ratio (GLR) test leads to the corresponding parametric test

$$t = \zeta^T \Sigma^{-1} \mathcal{J} \left(\mathcal{J}^T \Sigma^{-1} \mathcal{J} \right)^{-1} \mathcal{J}^T \Sigma^{-1} \zeta, \tag{5}$$

which follows asymptotically a χ^2 distribution with $\dim(\theta)$ degrees of freedom, and non-centrality parameter

$$\lambda = \delta^T (\mathcal{J}^T \Sigma^{-1} \mathcal{J}) \delta \tag{6}$$

in the damaged state. To decide between $\mathbf{H}_0$ and $\mathbf{H}_1$, the test variable t is compared to a threshold, which is set up such that the probability of false alarms is below some chosen level. In theory this choice can be made according to the χ^2 distribution of t from the reference system.

2.2. Problem statement

In the definition of the residual (2), only the Hankel matrix estimate $\widehat{\mathcal{H}}$ computed from the test data has been considered as a random variable, while the left null space S_0 associated to the reference state is considered to be computed from a model. Hence, both the residual distribution in (4) and the damage detection test (5) have been derived in previous works assuming that S_0 is deterministic.

However, this is not a realistic assumption. In practice, in the absence of a reference model, only an estimate $\widehat{S}_0$ of S_0 is usually available, which is computed from a Hankel matrix estimate $\widehat{\mathcal{H}}^{(0)}$ in the reference state, as suggested for applications e.g. in [35, 40, 46]. By nature, this Hankel matrix estimate is afflicted with statistical uncertainty and so is $\widehat{S}_0$. The related uncertainty may not be negligible, in particular for cases when the reference data set for the computation of $\widehat{\mathcal{H}}^{(0)}$ is relatively short. Consequently, the residual mean in the reference state is not exactly zero anymore under small errors in S_0, and the residual distribution in (4) may be incorrect. This can lead to an incorrect behavior of the damage detection test and to unwanted false alarms. To circumvent this problem, the uncertainty associated to the reference state is characterized in

this paper. Then, the appropriate damage detection tests are derived considering not only the uncertainties related to measurements in the test state but now also of the reference state.

3. Subspace-based damage detection method under uncertainty in reference

3.1. Residual definition and analysis of its distribution

In the residual definition (2), the theoretical left null space S_0 associated to the reference state is compared to the Hankel matrix estimate $\widehat{\mathcal{H}}$, which is computed on a data set of length N in the currently tested state. More realistically, an estimate $\widehat{S}_0$ of the theoretical null space is usually used, which is computed on a data set of length M in the reference state. Then, the data-driven subspace-based residual is defined as

$$\tilde{\zeta} = \sqrt{N}\,\mathrm{vec}(\widehat{S}_0^T\widehat{\mathcal{H}}). \tag{7}$$

The previous residual (2) depends only on one random variable, namely $\widehat{\mathcal{H}}$. Its mean in (4) is zero in the reference state, because the theoretical matrices yield $S_0^T\mathcal{H} = 0$ in the reference state. However, the product with the left null space estimate $\widehat{S}_0^T\mathcal{H}$ is just approximately but not exactly zero in the reference state, which has an impact on the distribution properties in (4). This impact is examined in the remainder of this section, and the distribution properties of the residual (7) with estimated reference null space are derived.

The distribution properties in (4) are based on the distribution of the Hankel matrix estimate $\widehat{\mathcal{H}}$ computed on test data of length N. Its exact distribution is unknown, but can be approximated as Gaussian. In fact, output data covariance estimates are asymptotically Gaussian [47], thus it is also the case for the vectorized Hankel matrices and associated matrices for many subspace methods [45]. Then, the distribution of $\widehat{\mathcal{H}}$ yields under the hypotheses (3)

$$\sqrt{N}\mathrm{vec}(\widehat{\mathcal{H}} - \mathcal{H}^{(0)}) \xrightarrow{d} \begin{cases} \mathcal{N}(0, \Sigma_{\mathcal{H}}) & \text{under } \mathbf{H}_0 \\ \mathcal{N}(\mathcal{J}_{\mathcal{H}}\,\delta, \Sigma_{\mathcal{H}}) & \text{under } \mathbf{H}_1 \end{cases} \tag{8}$$

where δ is defined in (3), and $\mathcal{J}_{\mathcal{H}}$ is the asymptotic sensitivity of $\mathrm{vec}(\mathcal{H})$ with respect to parameter θ (evaluated at θ_0). Note that an estimate of $\Sigma_{\mathcal{H}}$ can be easily obtained from the data via the sample covariance [45].

Now remark that (4) is a consequence of (8), since multiplication of (8) with deterministic matrix S_0^T in $\sqrt{N}\mathrm{vec}(S_0^T(\widehat{\mathcal{H}}-\mathcal{H}^{(0)}))$ is equal to residual ζ due to $S_0^T\mathcal{H}^{(0)} = 0$, which still yields an asymptotically Gaussian vector (with a different mean and covariance). This allows to state the residual distribution (4) without any knowledge on the theoretical limit value $\mathcal{H}^{(0)}$ that is unknown in practice. However, when replacing S_0 by its estimate $\widehat{S}_0$, this does not hold anymore since $\widehat{S}_0^T\mathcal{H}^{(0)} \neq 0$, and the central limit theorem in (4) would become incorrect. Since $\widehat{S}_0$ is a consistent estimate of S_0, the asymptotic mean of the residual is not affected, but the fact that $\widehat{S}_0^T\mathcal{H}^{(0)}$ is only approximately but not exactly zero leads to a modification of the residual

covariance. This computational inaccuracy has often been discarded in previous works [40], and empirical thresholds had to be used for the test (5). To achieve better performance for short data lengths and to define theoretically sound thresholds for detection, the distribution properties of $\tilde{\zeta}$ are derived, including the exact expression for its covariance for a correct computation of the corresponding damage detection test (5).

The estimate $\widehat{S}_0$ is computed on a dataset of length M in the reference state from $\widehat{\mathcal{H}}^{(0)}$. Hence, the error induced by replacing S_0 with $\widehat{S}_0$ depends on M, while the test data is computed on a data set of length N, which is the normalization factor of the residual (7). This implies that even if the asymptotic residual distribution depends on the test data length N, the impact of the reference data length M used to compute $\widehat{S}_0$ has to be taken into account, especially for small M. Recall that similarly to (8), the matrix estimate $\widehat{\mathcal{H}}^{(0)}$ is computed on a data set of length M, and it is asymptotically Gaussian with

$$\sqrt{M}\,\mathrm{vec}(\widehat{\mathcal{H}}^{(0)} - \mathcal{H}^{(0)}) \xrightarrow{d} \mathcal{N}(0, \Sigma_{\mathcal{H}}) \tag{9}$$

when $M \to \infty$, where $\Sigma_{\mathcal{H}}$ is the asymptotic Hankel matrix covariance that is the same as in the reference state under the assumption of unchanged noise properties [5, 33]. Then, the data-driven residual (7) is analyzed as a function of both random variables $\widehat{S}_0$ (derived from $\widehat{\mathcal{H}}^{(0)}$ in the reference state) and $\widehat{\mathcal{H}}$ (computed in the test state), from which it inherits its distribution properties. This function is denoted by $g(\hat{h}) = \mathrm{vec}(\widehat{S}_0^T\widehat{\mathcal{H}})$, where

$$\hat{h} = \begin{bmatrix} \mathrm{vec}(\widehat{\mathcal{H}}^{(0)}) \\ \mathrm{vec}(\widehat{\mathcal{H}}) \end{bmatrix}, \text{ and } h = \begin{bmatrix} \mathrm{vec}(\mathcal{H}^{(0)}) \\ \mathrm{vec}(\mathcal{H}^{(0)}) \end{bmatrix},$$

with $g(h) = 0$. With the statistical delta method [48], the asymptotically Gaussian distribution properties of $\hat{h}$ are propagated to $g(\hat{h})$, i.e. to the residual $\tilde{\zeta} = \sqrt{N}(g(\hat{h}) - g(h))$. For this, the joint asymptotic distribution of $\widehat{\mathcal{H}}^{(0)}$ and $\widehat{\mathcal{H}}$ in $\hat{h}$ is detailed first. Since $\widehat{\mathcal{H}}^{(0)}$ is computed on a data set of length M, but the residual is normalized with data length N of the test state, the ratio $c = \frac{N}{M}$ is introduced. Multiplication of $\sqrt{c}$ to the asymptotic distribution properties of $\widehat{\mathcal{H}}^{(0)}$ in (9) leads to

$$\sqrt{M}\,\sqrt{\tfrac{N}{M}}\mathrm{vec}(\widehat{\mathcal{H}}^{(0)} - \mathcal{H}^{(0)}) \xrightarrow{d} \mathcal{N}(0, c\Sigma_{\mathcal{H}}). \tag{10}$$

Since $\widehat{\mathcal{H}}^{(0)}$ and $\widehat{\mathcal{H}}$ are computed on different data sets in the reference and in the test states, respectively, they can be considered as independent. Then, their joint distribution follows from (8) and (10) as

$$\sqrt{N}(\hat{h} - h) = \sqrt{N}\left(\begin{bmatrix} \mathrm{vec}(\widehat{\mathcal{H}}^{(0)}) \\ \mathrm{vec}(\widehat{\mathcal{H}}) \end{bmatrix} - \begin{bmatrix} \mathrm{vec}(\mathcal{H}^{(0)}) \\ \mathrm{vec}(\mathcal{H}^{(0)}) \end{bmatrix}\right) \xrightarrow{d} \begin{cases} \mathcal{N}\left(\begin{bmatrix} 0 \\ 0 \end{bmatrix}, \begin{bmatrix} c\Sigma_{\mathcal{H}} & 0 \\ 0 & \Sigma_{\mathcal{H}} \end{bmatrix}\right) & \text{under } \mathbf{H}_0 \\ \mathcal{N}\left(\begin{bmatrix} 0 \\ \mathcal{J}_{\mathcal{H}}\delta \end{bmatrix}, \begin{bmatrix} c\Sigma_{\mathcal{H}} & 0 \\ 0 & \Sigma_{\mathcal{H}} \end{bmatrix}\right) & \text{under } \mathbf{H}_1 \end{cases} \tag{11}$$

With this result and the first-order Taylor expansion

$$g(\hat{h}) = g(h) + \mathcal{J}_g(\hat{h} - h) + o(||\hat{h} - h||), \quad \mathcal{J}_g = \frac{\partial g(h)}{\partial h}, \tag{12}$$

the delta method [48] states that $\tilde{\zeta} = \sqrt{N}(g(\hat{h}) - g(h))$ is asymptotically Gaussian with

$$\tilde{\zeta} \xrightarrow{d} \begin{cases} \mathcal{N}(0, \tilde{\Sigma}) & \text{under } \mathbf{H}_0 \\ \mathcal{N}(\mathcal{J}\,\delta, \tilde{\Sigma}) & \text{under } \mathbf{H}_1 \end{cases} \tag{13}$$

where the asymptotic covariance is

$$\tilde{\Sigma} = \mathcal{J}_g \begin{bmatrix} c\Sigma_{\mathcal{H}} & 0 \\ 0 & \Sigma_{\mathcal{H}} \end{bmatrix} \mathcal{J}_g^T, \tag{14}$$

which is developed in the following section. Note that it is the same under both hypotheses due to the close hypotheses definition (3), similar to (4). In (13), δ is the change vector that has been defined in (3), and the residual sensitivity $\mathcal{J}$ is the same as in (4). Its computation depends on the used system parametrization and is detailed e.g. in [5, 39].

3.2. Covariance computation

The asymptotic residual covariance $\tilde{\Sigma}$ in (14) requires the evaluation of the derivative $\mathcal{J}_g$ of the residual with respect to h in (12), i.e. with respect to the vectorized Hankel matrices corresponding to the reference and to the test states. This is developed in detail in the Appendix, where it is shown that the respective derivatives yield

$$\mathcal{J}_g = \begin{bmatrix} \mathcal{J}_{\tilde{\zeta},\mathcal{H}^{(0)}} & \mathcal{J}_{\tilde{\zeta},\mathcal{H}} \end{bmatrix} = \begin{bmatrix} -V_1 V_1^T \otimes S_0^T & I_{qr} \otimes S_0^T \end{bmatrix}, \tag{15}$$

where V_1 defines the row space of $\mathcal{H}^{(0)}$, and $\otimes$ denotes the Kronecker product. Finally, the asymptotic covariance of the residual follows from (14) as

$$\tilde{\Sigma} = c\Sigma_1 + \Sigma_2, \tag{16}$$

where $\Sigma_1 = \mathcal{J}_{\tilde{\zeta},\mathcal{H}^{(0)}} \Sigma_{\mathcal{H}} \mathcal{J}_{\tilde{\zeta},\mathcal{H}^{(0)}}^T$ is related to the uncertainty in $\widehat{S}_0$, and $\Sigma_2 = \mathcal{J}_{\tilde{\zeta},\mathcal{H}} \Sigma_{\mathcal{H}} \mathcal{J}_{\tilde{\zeta},\mathcal{H}}^T$ is related to the uncertainty of $\widehat{\mathcal{H}}$, i.e. to the test state.

With these developments, the theoretical asymptotic covariance of the residual is characterized. Based on the obtained expression in (16), its estimate can be obtained from actual measurements as follows. From measurements in the reference state (of length M), the estimates $\widehat{S}_0$ and $\widehat{V}_1$ are available from $\widehat{\mathcal{H}}^{(0)}$, e.g. from the SVD

$$\widehat{\mathcal{H}}^{(0)} = \begin{bmatrix} \widehat{U}_1 & \widehat{U}_2 \end{bmatrix} \begin{bmatrix} \widehat{D}_1 & 0 \\ 0 & \widehat{D}_2 \end{bmatrix} \begin{bmatrix} \widehat{V}_1^T \\ \widehat{V}_2^T \end{bmatrix} \tag{17}$$

as $\widehat{S}_0 = \widehat{U}_2$, where $\widehat{U}_1$ contains the first n columns of the left singular vector matrix associated to the non-zero singular values in $\widehat{D}_1 \in \mathbb{R}^{n \times n}$ and $\widehat{U}_2$ contains the remaining columns associated to $\widehat{D}_2 \approx 0$. With these matrices, an estimate of $\mathcal{J}_g$ can be computed in (15). The estimate of the Hankel matrix covariance $\widehat{\Sigma}_{\mathcal{H}}$ can be computed as the sample covariance from data blocks of the available data, as detailed e.g. in

[5, 45], and estimates $\widehat{\Sigma}_1$ and $\widehat{\Sigma}_2$ are obtained analogously to (16). With the data length N of the data set in the test state, $c = \frac{N}{M}$ and the estimate of the residual covariance is obtained as

$$\widehat{\tilde{\Sigma}} = \tfrac{N}{M}\widehat{\Sigma}_1 + \widehat{\Sigma}_2. \tag{18}$$

Hence, when the data length M to compute the reference matrix $\widehat{S}_0$ is large with respect to the data length N for computing $\widehat{\mathcal{H}}$ from the current test data, the residual covariance depends more strongly on $\widehat{\mathcal{H}}$ (related to $\widehat{\Sigma}_2$), which is the more uncertain part in the residual computation in this case. Thus, the covariance contribution $\widehat{\Sigma}_1$ related to the reference matrix gets weaker when long data sets are available in the reference state, which is reflected in (18) where $\frac{N}{M}$ is small in this case. On the other side, when M is small compared to N, the contribution to the residual covariance of the uncertainty related to the reference matrix $\widehat{S}_0$ is large compared to the uncertainty of $\widehat{\mathcal{H}}$ computed from the test data. Then, $\frac{N}{M}$ is large and indeed the contribution of $\widehat{\Sigma}_1$ in (18) is larger. Notice finally that this term is the contribution of the new covariance scheme of this paper. To neglect it in the residual covariance (18), as in previous studies, the reference data length M needs to be significantly larger than the test data length N, by some orders of magnitude, as will be illustrated later in the paper.

3.3. Computation of test statistic

In the previous sections, the asymptotic distribution of the residual $\tilde{\zeta}$ has been characterized, with the central limit theorem in (13) and the estimation of the respective covariance $\tilde{\Sigma}$ in Section 3.2. The residual sensitivity $\mathcal{J}$ and its estimation has been detailed in previous works, e.g. in [5, 39]. Finally, the GLR test for hypotheses (3) based on (13) writes

$$\tilde{t} = \tilde{\zeta}^T\tilde{\Sigma}^{-1}\mathcal{J}\left(\mathcal{J}^T\tilde{\Sigma}^{-1}\mathcal{J}\right)^{-1}\mathcal{J}^T\tilde{\Sigma}^{-1}\tilde{\zeta} \tag{19}$$

analogously to (5), and is consistently computed when replacing $\mathcal{J}$ and $\tilde{\Sigma}$ by their respective estimates. The test statistic $\tilde{t}$ is asymptotically χ^2 distributed with $\dim(\theta)$ degrees of freedom and non-centrality parameter

$$\tilde{\lambda} = \delta^T(\mathcal{J}^T\tilde{\Sigma}^{-1}\mathcal{J})\delta \tag{20}$$

in the damaged state.

4. Numerical validation

The properties of the developed damage detection test (19) are validated on simulation data of a mass-spring-damper system, and compared to the conventional test computation where the covariance contribution Σ_1 related to the left null space estimate in the reference state is neglected. The mass-spring-damper (Fig. 1) is defined by eight masses with $m_1 = m_3 = m_5 = m_7 = 1, m_2 = m_4 = m_6 = m_8 = 2$, spring stiffnesses

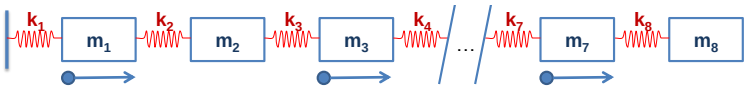

Figure 1: Mass-spring chain with four sensors.

$k_1 = k_3 = k_5 = k_7 = 200, k_2 = k_4 = k_6 = k_8 = 100$, and classical damping with a damping ratio of 2% for all modes. In the damaged state the stiffness of the third spring is decreased.

For each simulated data set, the system is excited by random white noise loads at masses m_1, m_3, m_5, m_7. Velocity data is recorded at the same four positions and sampled with 20 Hz, considering an additional measurement noise with 5% standard deviation of the signal.

The behavior of the developed method is examined in Monte Carlo experiments and compared to its expected theoretical properties for validation and performance evaluation. Hereby, three typical cases for the system parametrization θ are considered [49], namely structural parameters in Section 4.1, modal parameters in Section 4.2, and no parametrization in the corresponding non-parametric damage detection test in Section 4.3. The experiments are carried out with the main focus on different reference data lengths M to examine the influence of the uncertainty in $\widehat{S}_0$ related to the reference state within the new and the conventional test computation. The performance is evaluated by means of the probability of detection (POD) for different damages in the third spring. Each Monte Carlo experiment contains 1,000 simulations of reference data sets and of test data sets for the computation of the reference null space $\widehat{S}_0$ and the test Hankel matrix $\widehat{\mathcal{H}}$, respectively. Both these terms are afflicted with uncertainty in the computation of the residual $\tilde{\zeta}$ in (7), which is analyzed for different data lengths and system states for damage detection. In the test computation, the estimation of the asymptotic Hankel matrix covariance $\Sigma_{\mathcal{H}}$ is not part of the uncertainty analysis, and it is assumed that it is appropriately estimated on reference data as in [5].

4.1. Detection with focus on structural parameter changes

In a first example, the system is parameterized by the stiffness of the eight springs, i.e. $\theta = [k_1\ k_2\ \ldots\ k_8]^T$. The residual sensitivity $\mathcal{J}$ used in the conventional test (5) as well as in the new test (19) contains the derivatives of the residual regarding these structural parameters. It is obtained by first deriving the residual with respect to the modal parameters, and then the modal parameters with respect to the structural parameters, as detailed e.g. in [38, 39]. In its estimation, the reference null space $\widehat{S}_0$ is required, which is computed anew in each Monte Carlo simulation. Since the system is parametrized by eight parameters, the χ^2-distributed test statistics have $\mu = \text{rank}(\mathcal{J}^T\Sigma^{-1}\mathcal{J}) = 8$ degrees of freedom and thus their expected value in the reference state is 8.

Fig. 2 shows the histograms of the conventional test (left) and the new test computation (right), for both the reference and the damaged states. The reference null space estimate $\widehat{S}_0$ is computed from data sets of length $M = 50{,}000$, and the Hankel matrix estimate $\widehat{\mathcal{H}}$ is computed from data sets of length $N = 100{,}000$.

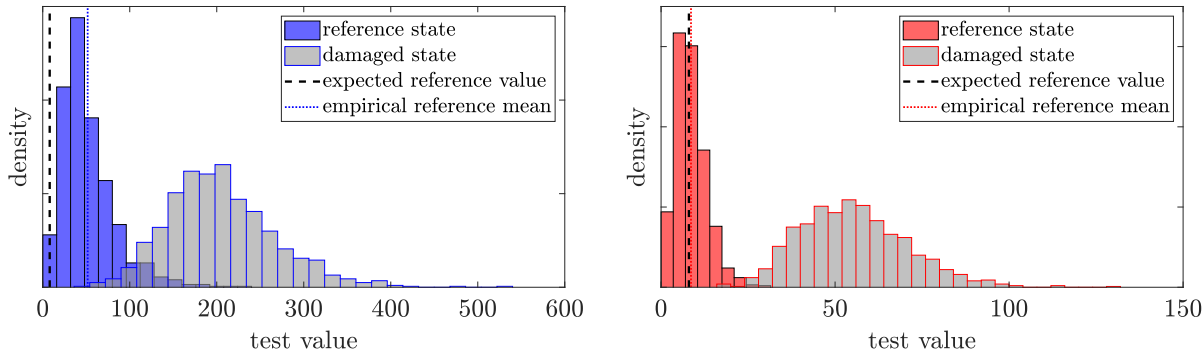

Figure 2: Histograms of test statistics with conventional covariance computation ($\Sigma_1 = 0$, left) and new test (right).

In the damaged state the stiffness of spring 3 is decreased by 1.4%. In the conventional test in Fig. 2 (left), the uncertainty related to $\widehat{S}_0$ is not taken into account, and Σ_1 in the covariance computation in (18) is set to zero. The mean of the test values in the reference state is $\hat{\mu} = 53$, which differs clearly from its expected reference value $\mu = 8$, and the spread of the test values is large. This is due to considerable uncertainty in the reference null space estimation, and consequently to a shift in the residual mean already in the reference state, as explained in Section 2.2. In the new test computation in Fig. 2 (right), all relevant uncertainties are taken into account, and the test values in the reference state are well centered around the theoretical value $\mu = 8$. In contrast to the test results obtained by the conventional test, the distribution of the new test is narrower and there is less overlap between the values from the reference and the damaged states.

In Fig. 3, the test value means in the reference state are shown for both tests when the data length M for the estimation of the reference null space increases. The new test yields almost constant test value means for an increasing data length M, matching its theoretical value already for very short data lengths. With the conventional test, the test value mean is much higher for short data in the reference state, and it approaches its theoretical expected value only for longer data sets. This is a consequence of less uncertainty in the estimate $\widehat{S}_0$ when using longer data sets for its computation, where the estimate approaches its theoretical value $\widehat{S}_0 \to S_0$, and thus the theoretical properties of the conventional test are approached.

The impact of the new test computation on the probability of detecting damage is demonstrated in Fig. 4. The POD for both the conventional and the new tests is displayed for two different data lengths $M = 50{,}000$ (left) and $M = 500{,}000$ (right) for the reference null space estimation. To determine the POD in a practical way, an empirical threshold is determined from the histogram of test values in the undamaged case allowing a maximum of 1% false alarms. Damage is detected if the test value exceeds this threshold.

In Fig. 4 (left) it can be seen that the performance of the new test improves significantly with respect to the conventional test for small damage and small M. The POD reflects how well the distributions of the test values are separated between the reference and damaged states. In the conventional test computation,

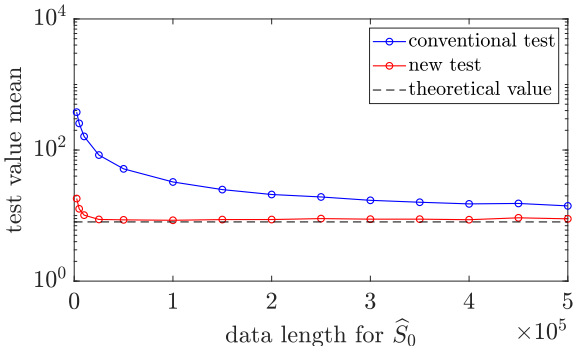

Figure 3: Mean of test statistic in the reference state, with structural system parametrization.

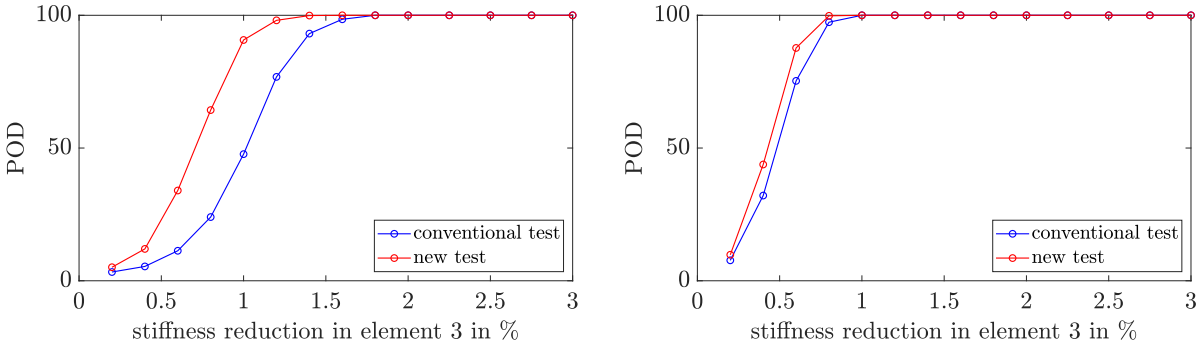

Figure 4: Test performance with conventional ($\Sigma_1 = 0$) and new covariance computation, with structural system parametrization. Reference null space computation with data length $M = 50{,}000$ (left) and $M = 500{,}000$ (right).

a bias is introduced in the residual mean, which leads to a non-centrality of the test distribution already in the reference state. Then, the mean is higher than the theoretical value as shown in Fig. 3, implying also a larger spread of the χ^2-distribution due to its distribution properties. Finally, this leads to more overlap between the distributions in the reference and damaged states and thus lower POD with the conventional test, whereas the new test yields a distribution with less spread in the reference state (being at the theoretical mean value) and less overlap with the distribution in the damaged state. Larger damage leads to higher non-centrality parameters, and at a certain point the non-centrality parameter is large enough to avoid an overlap of the distributions of the reference and the damaged states for both test methods.

If a long data set of length $M = 500{,}000$ is used, the reference null space estimate is closer to its theoretical value. Then its uncertainty becomes small, the related covariance contribution $\frac{N}{M}\Sigma_1$ in (18) decreases and both tests perform similarly, as shown in Fig. 4 (right).

Comparing Fig. 4 (left) with Fig. 4 (right), it can be seen that the POD increases for the higher value of M. This is examined further in Fig. 5, where the POD of an example damage case is shown for different reference data lengths M. The POD increases with increasing M for both tests. The reason for the

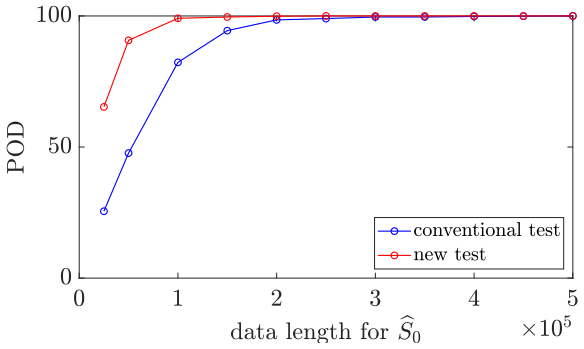

Figure 5: Test performance with conventional ($\Sigma_1 = 0$) and new covariance computation for different reference data lengths M, with 1% stiffness reduction in spring 3 and using structural system parametrization.

increasing POD in the conventional test is the decreasing mean of the test distribution in the reference state as shown in Fig. 3, which approaches its theoretical value and leads to a better separation to the distribution in the damaged state when M increases. In the new test, the test distribution in the reference state is independent of M, and the POD increases with increasing M since the non-centrality parameter increases: with increasing M there is less uncertainty on the reference null space, which is reflected in the decreasing covariance contribution $\frac{N}{M}\Sigma_1$ in (18). This leads qualitatively to a smaller residual covariance $\tilde{\Sigma}$, a larger inverse $\tilde{\Sigma}^{-1}$ and thus a larger non-centrality parameter $\tilde{\lambda}$ in (20). As can be seen in Fig. 5, the new test outperforms the conventional test in particular for small data lengths. The behavior of both tests becomes closer as M increases when the uncertainty related to the reference state becomes negligible.

The previous results have illustrated that the behavior of the new test is close to the expected theoretical properties, whereas the conventional test shows a somewhat unpredictable behavior for small reference data lengths M. Moreover, the test performance of the new test has shown to be better in terms of the POD than the performance of the conventional test for small M. Hereby, the POD was determined by setting up empirical thresholds in the reference state in order to allow a fair and practical comparison between both tests. In the following, the behavior of the tests in the reference state is further analyzed with regards to the theoretical thresholds of the distributions. This is particularly relevant for cases when only few data sets are available in the reference state, preventing the definition of empirical thresholds.

In Fig. 6, the histograms of the conventional test (left) and the new test (right) are presented for increasing data length M in the reference state. For the conventional test in Fig. 6 (left), the histograms differ significantly for the different data lengths M and their mean differs from the theoretical value. In this case it would be impossible to set up a threshold based on the expected distribution properties. The new test, however, yields similar histograms independently of the data length M in Fig. 6 (right) whose mean matches the theoretical value.

Besides the possibility to define a theoretical threshold with the new test independently of the available

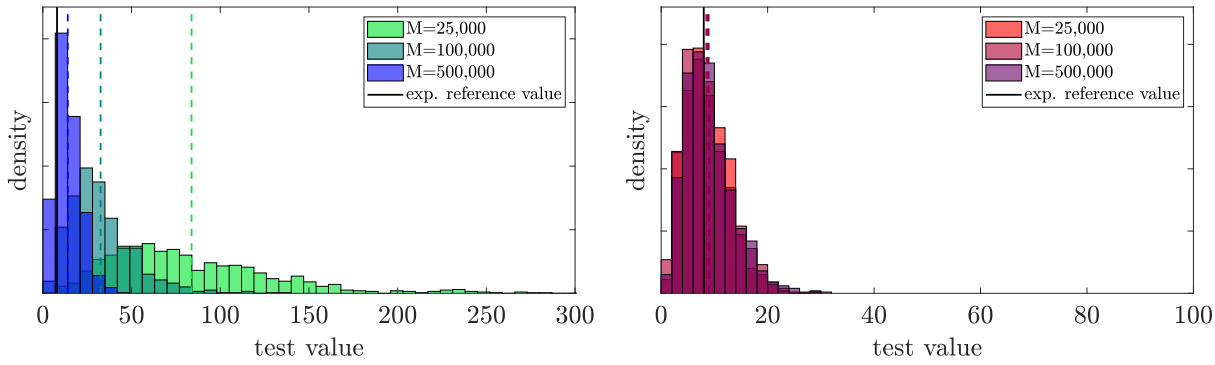

Figure 6: Histograms of the test statistic of the conventional (left) and the new test (right) in the undamaged reference state, computed with different reference data lengths M and $N = 100{,}000$.

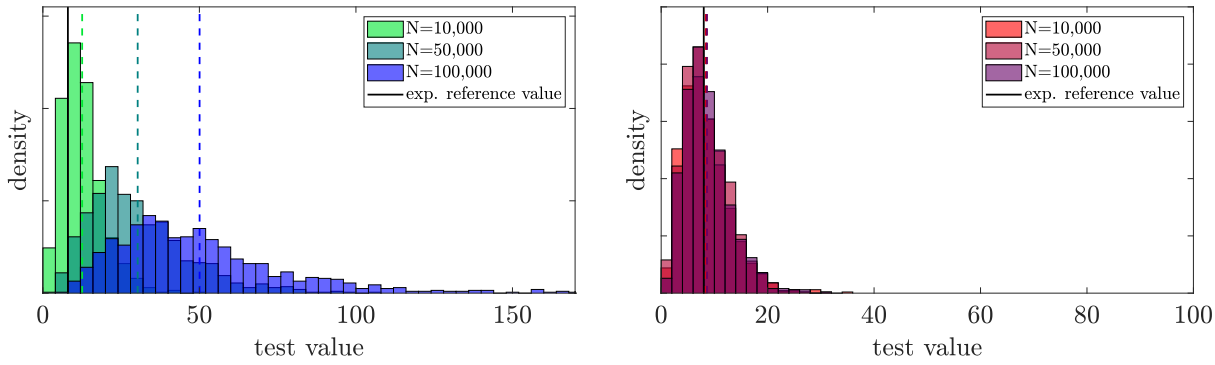

Figure 7: Histograms of the test statistic of the conventional (left) and the new test (right) in the undamaged reference state, computed different test data lengths N and $M = 50{,}000$.

data length M in the reference state, its behavior is also consistent when applied to testing data of different lengths N as shown in Fig. 7 (right), whereas the histograms of the conventional test in Fig. 7 (left) differ significantly. This is due to the bias that is introduced in the conventional test when neglecting the uncertainty on the reference null space. In practice, this means that the conventional test is subject to false alarms in the reference state when evaluated on testing data of different lengths, which is not the case for the new test.

These results show that for the conventional test, a threshold has to be determined empirically from (sufficient) test data. Its value depends on the data lengths M and N, and moreover N has to be constant in the monitoring phase. The new test, however, allows the definition of a fixed threshold, which can be based on the theoretical distribution properties and thus be computed explicitly a priori. This is very valuable in particular when only few data is available in the reference state.

This section has demonstrated that the application of these damage detection methods shows good

accordance with the theoretically expected behavior if the uncertainty related to the reference data is either correctly considered in the residual covariance, or if this uncertainty is negligible due to sufficiently long reference data sets. In the application of the methods, the system parametrization θ was chosen as the structural system parameters. While such a parametrization is quite powerful also for further damage diagnosis [39, 49], it may not be provided easily and requires usually a finite element model. This motivates for a simpler but still complete parameterization, such as the modal parameters in the following section.

4.2. Detection with focus on modal parameter changes

When considering the modal parametrization of the system, parameter vector θ can be defined by the real and imaginary parts of the eigenvalues and mode shapes of system (1) [4, 34]. They can be easily obtained from data in the reference state, and the residual sensitivity matrix $\mathcal{J}$ has been detailed e.g. in [5, 34]. The dimension of the parameter vector is $2mr$. Thus, the number of degrees of freedom of the χ^2-distributed test statistic and its theoretical expected value in the reference state is $\text{rank}(\mathcal{J}^T\Sigma^{-1}\mathcal{J}) = 2mr$. For the considered 8-mass-spring-damper with $m = 8$ modes and $r = 4$ sensors, this computes to $2mr = 64$.

Using this parametrization, the conventional and new tests have been computed again with the Monte Carlo simulations from the previous section for different reference data lengths M. Similarly to Fig. 3, Fig. 8 shows the evolution of the test means when the reference data length M increases. The mean of the new test is close to its theoretical value even for short data length M as expected, since the uncertainty of the reference null space estimate is correctly taken into account. The conventional test needs much longer data sets to approach the expected value.

The performance of the tests in terms of the POD is compared in Fig. 9 for small damage in spring 3, using short reference data with $M = 50{,}000$ in Fig. 9 (left) and longer data sets with $M = 500{,}000$ (right). In both cases, the POD increases with the new test when the damage is small, until it reaches 100%. Using longer data sets in the reference state (right) increases the POD, and reduces the difference between the respective POD of both tests due to a better estimate of the reference null space with less uncertainty. In

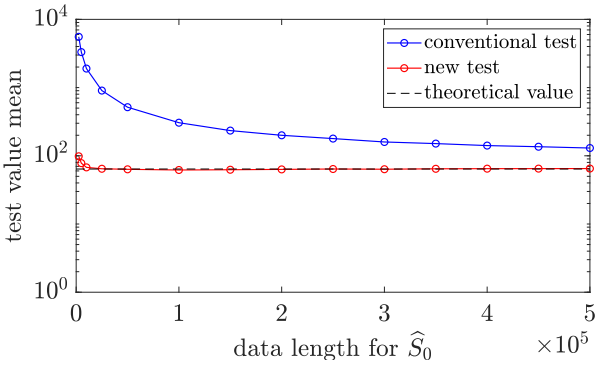

Figure 8: Mean of test statistic, with modal system parametrization.

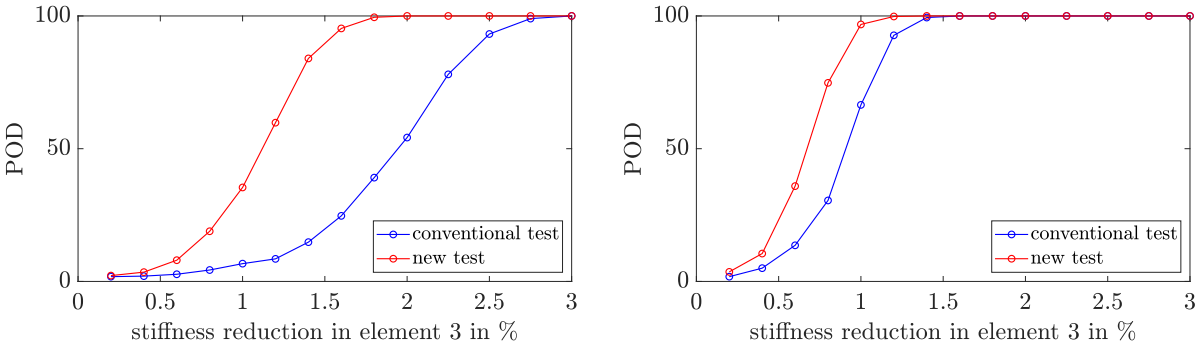

Figure 9: Test performance with conventional ($\Sigma_1 = 0$) and new covariance computation, with modal system parametrization. Reference null space computation with data length $M = 50{,}000$ (left) and $M = 500{,}000$ (right).

this case, the difference between the conventional and the new test performance is not as small as in Fig. 4 (right) when using the structural parametrization. This is due to the larger number of degrees of freedom and wider spread of the test distribution under the modal parametrization in this application. However, this also indicates that even with a long reference data length of $M = 500{,}000$ there is non-negligible uncertainty in the reference null space estimate that should be taken into account to achieve an optimal test performance.

4.3. Non-parametric detection

Finally, the damage detection tests are applied without focussing on a particular system parametrization θ, which corresponds to a direct detection of changes in the residual and $\mathcal{J} = I$ [5, 49]. Then, the conventional and the new tests in (5) and (19) boil down to $t = \zeta^T \Sigma^{-1} \zeta$ and $\tilde{t} = \tilde{\zeta}^T \tilde{\Sigma}^{-1} \tilde{\zeta}$, respectively, and the number of degrees of freedom of their χ^2 distribution is the theoretical rank of the residual covariance. These non-parametric tests are attractive due to their simplicity, and may be preferred e.g. when the identification of the modal parameters in the reference state of the system is inconvenient.

The POD of both the conventional and the new test are displayed in Fig. 10, for the same reference data lengths M as above, i.e. $M = 50{,}000$ and $M = 500{,}000$. Similarly to the parametric cases, the POD improves for the new test compared to the conventional test, and both tests show a better and closer performance for large M. They also coincide for large damage with a recurring advantage for the new test.

Compared to the test performance of the parametric tests in Figs. 4 and 9, the POD in the non-parametric test is lower. This can be explained from the larger number of degrees of freedom of the χ^2-distribution of the test statistic in the non-parametric case, which leads to its wider spread and is coherent with the findings in [49].

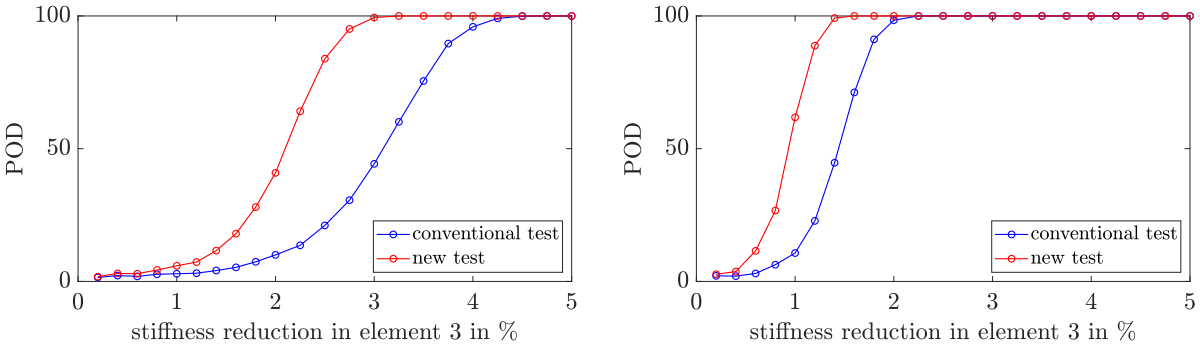

Figure 10: Test performance with conventional ($\Sigma_1 = 0$) and new covariance computation with non-parametric test. Reference null space computation with data length $M = 50{,}000$ (left) and $M = 500{,}000$ (right).

5. Application to experimental data

In the previous section the developed damage detection test has been validated on simulation data, where its behavior was shown to be coherent with its theoretically expected properties thanks to the consideration of the uncertainty related to the reference data. Moreover, it has shown to be robust for different data lengths, with an increased performance especially for short reference data lengths compared the conventional test. In this section, the tests are applied to a laboratory steel frame structure for an evaluation of the test performance on experimental data.

The considered steel frame structure represents a scaled two-dimensional section of a jacket-type support structure of an offshore wind turbine and is shown in Fig. 11. It is made of steel pipe components with an I-sectional steel beam on the top. At the bottom the structure is screwed to the floor. At the top the structure is fixed perpendicular to the in-plane-direction. The parts are mainly welded, except for the area

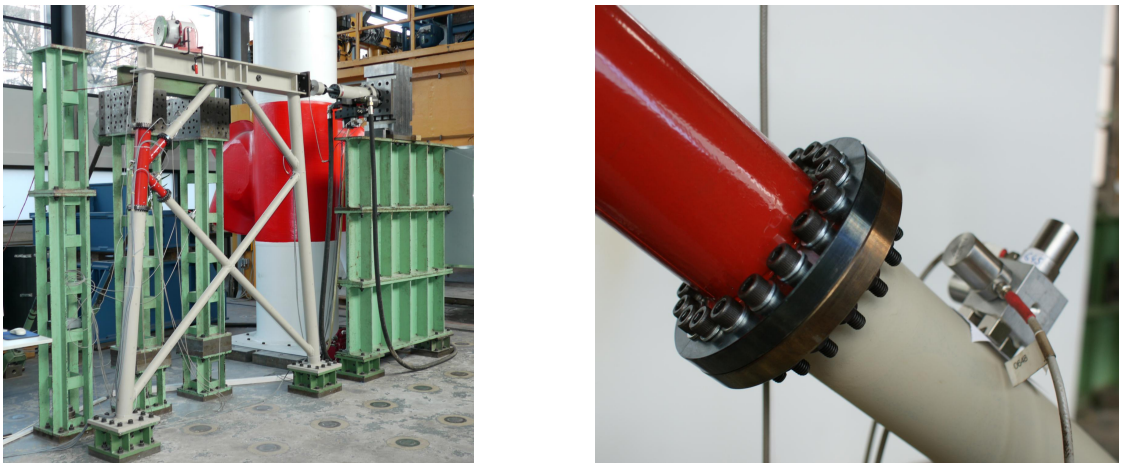

Figure 11: Laboratory testing structure (left) and reversible damage detail (right).

where a reversible damage can be introduced. This damage area is defined by a K-node, which is fixed to the structure by means of screwed end plates (see Fig. 11 right). Loosening the screws successively, the progress of a crack-like damage can be introduced. A high number of bolts are used to provide a high resolution of the induced stiffness loss.

An electrodynamic shaker excites the structure with a random white noise signal in the range of 10 to 1000 Hz and accelerations at nine locations are measured with a sampling rate of 2500 Hz. The excitation direction is approximately 30° rotated out of the in-plane-direction. Further details of the test setup can be found in [50].

The damage location, where the bolts are loosened, is set to be at the lower brace. In the reference state all bolts are screwed tight. For increasing damage, 1, 2, 3, 5 or 7 bolts are unscrewed. The loosening of 3, 5, and 7 bolts represents a reduction of the moment of inertia of 1%, 10%, and 30%, respectively.

For the damage detection test, the recorded data is separated into eight data sets with $N = 20{,}480$ data points each (about 8 seconds) for each system state. For the reference system state, a part of the first data set of the undamaged state is used to compute the reference matrix $\widehat{S}$, as well as the residual covariance $\widehat{\Sigma}$ and $\widehat{\tilde{\Sigma}}$ for the conventional and the new test, respectively. The remaining data sets are then used for damage detection with the non-parametric test procedure. This is the most convenient test setup with a high practicability, as the system identification step is avoided. Since no parametrization is used, the number of degrees of freedom of the test is related to the rank of the converged covariance matrices Σ or $\tilde{\Sigma}$ of the tests, respectively, which however cannot be evaluated with limited data. Nevertheless, an upper bound is given by their size, which is limited by the number of data blocks in their estimation [5]. In this application, 500 data blocks have been used for the computation of $\widehat{\Sigma}$ and $\widehat{\tilde{\Sigma}}$, hence the degrees of freedom of the χ^2 test distributions are limited by 500, where the threshold allowing for 1% false positive alarms is at 576.

Fig. 12 shows the test values in the undamaged reference state of the conventional test (left) and when the uncertainty of the reference is considered in the new test procedure (right) for different data lengths M.

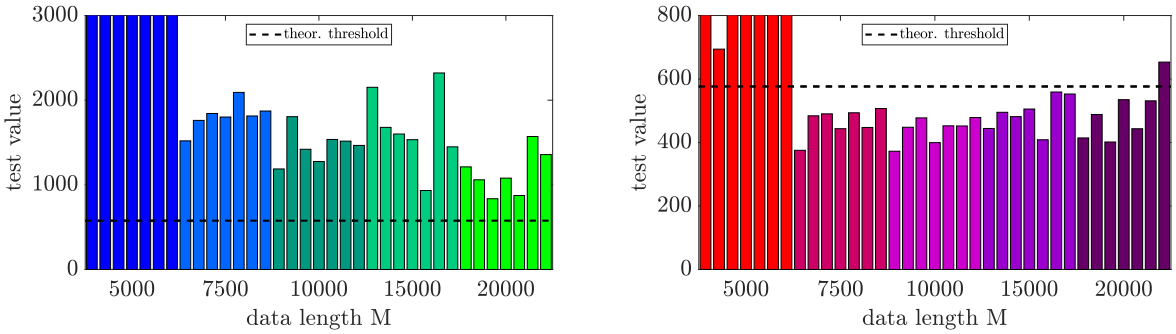

Figure 12: Test values of the conventional (left) and the new test (right) in the undamaged reference state computed with different reference data lengths M.

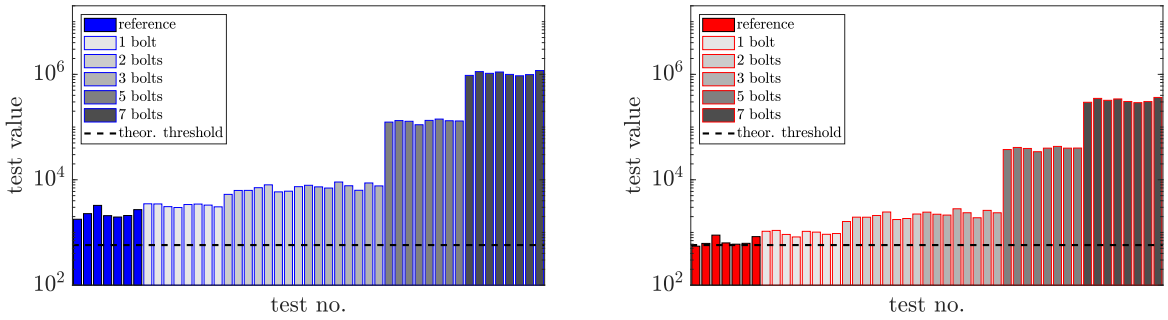

Figure 13: Test values of the conventional (left) and the new test (right) in the reference and at different damaged states.

In accordance with the numerical evaluation in Section 4 the conventional test leads to test values clearly above the threshold in Fig. 12 (left). Moreover, the test values depend on the reference data length M used for the computation of the reference null space and the covariance matrix, as they tend to decrease with increasing M as can similarly be seen in Fig. 3. With the new testing method only the test values for the very short data length $M = 5{,}000$ are above the threshold in Fig. 12 (right), and indeed it can also be observed in Fig. 3 that the test value mean has not converged yet for very small M. For the other used data lengths, the test values are consistently below the theoretical threshold and do not show any dependence of M.

The test values in the different system states are presented in Fig. 13 for both tests, where the reference data length $M = 15{,}000$ was chosen. Both tests are able to indicate changes in the system by an increase in the test values, even for damages below 1% stiffness reduction. All damages can be detected reliably using the theoretical threshold with the new test, while the conventional test method fails to recognize the healthy state with the theoretical threshold.

6. Conclusion

In this paper, the estimation uncertainties stemming from reference data have been analyzed for an established damage detection residual and the associated statistical test. In the considered residual, a Hankel matrix containing the system's output covariances computed from test data is confronted to its left null space, which is now estimated from reference data in the healthy state, instead of assuming it to be perfectly known from a model. While previously only the statistical uncertainties related to the test data have been considered, it is shown in this paper that the estimation uncertainties related to the reference data are non-negligible especially when the reference data is of short length. It has been shown that neglecting these uncertainties can lead to a considerable deviation from the theoretically expected test behavior. This can lead to false alarms and makes it impossible to set thresholds between healthy and damaged states based on the expected statistical distribution of the test. However, with a proper test design that takes into

account both the uncertainties related to the reference and to the test data, the developed damage detection test shows a correct and predictable statistical behavior. It is stable for different data lengths, and allows a reliable definition of thresholds a priori. This is in particular valuable in practice for cases where only short data is available in the reference state of a structure. The developed approach has been validated extensively on simulation data, where it has also been illustrated that its performance in terms of the POD is superior compared to the case where the uncertainties related to the reference data are neglected. Finally, the approach has been successfully applied to experimental data from a laboratory steel frame structure under progressive damage.

Appendix A. Development of the asymptotic residual covariance

The sensitivity matrix $\mathcal{J}_g$ in (12) is required for the evaluation of the asymptotic covariance $\tilde{\Sigma}$ of the data-driven residual in (14). For this, the derivative of $\text{vec}(S_0^T\mathcal{H})$ needs to be evaluated with respect to $\text{vec}(\mathcal{H}^{(0)})$ (S_0 depends on $\mathcal{H}^{(0)}$) and with respect to $\text{vec}(\mathcal{H})$. These derivatives are obtained through first-order perturbations $\Delta(\cdot)$, which is convenient for asymptotically Gaussian variables, as e.g. in [45]. For vector-valued functions $\hat{Y} = f(\hat{X})$ of some estimate $\hat{X}$ of X, a first-order Taylor approximation yields $f(\hat{X}) \approx f(X)+\mathcal{J}_{Y,X}(\hat{X}-X)$, or simply $\Delta Y \approx \mathcal{J}_{Y,X}\Delta X$, where $\mathcal{J}_{Y,X}$ is the derivative of f, and $\Delta X = \hat{X}-X$ for $\hat{X}$ close to X. With this notation, it is the goal to determine $\mathcal{J}_g$ through the relationship

$$\text{vec}(\Delta(S_0^T\mathcal{H})) = \mathcal{J}_g \begin{bmatrix} \text{vec}(\Delta\mathcal{H}^{(0)}) \\ \text{vec}(\Delta\mathcal{H}) \end{bmatrix}. \tag{A.1}$$

Using the relation $\text{vec}(AXB) = (B^T \otimes A)\text{vec}(X)$, where $\otimes$ is the Kronecker product, it holds

$$\begin{aligned} \text{vec}(\Delta(S_0^T\mathcal{H})) &= \text{vec}(\Delta S_0^T\mathcal{H}) + \text{vec}(S_0^T\Delta\mathcal{H}) \\ &= \mathcal{J}_{\tilde{\zeta},S_0}\,\text{vec}(\Delta S_0) + \mathcal{J}_{\tilde{\zeta},\mathcal{H}}\text{vec}(\Delta\mathcal{H}), \end{aligned} \tag{A.2}$$

with $\mathcal{J}_{\tilde{\zeta},S_0} = (\mathcal{H}^T \otimes I_s)\mathcal{P}_{t,s}$, $\mathcal{J}_{\tilde{\zeta},\mathcal{H}} = I_{qr} \otimes S_0^T$, $\mathcal{P}_{a,b}$ is a permutation matrix such that $\text{vec}(X^T) = \mathcal{P}_{a,b}\text{vec}(X)$ for a matrix $X \in \mathbb{R}^{a\times b}$ [51] and t and s are the number of rows and columns of S_0, respectively. Furthermore, a perturbation ΔS_0 is linked to $\Delta\mathcal{H}^{(0)}$ as follows. First, $\Delta\mathcal{H}^{(0)}$ is propagated to the column space U_1 in SVD (17) by [52]

$$\Delta U_1 = U_1 R + U_2 U_2^T \Delta\mathcal{H}^{(0)}\ V_1 D_1^{-1},$$

where R is a matrix that will be canceled in the following, and matrices U_1, U_2, D_1 and V_1 are the limit values of the respective matrices in SVD (17). In the vectorized form it follows

$$\text{vec}(\Delta U_1) = (I_n \otimes U_1)\ \text{vec}(R) + (D_1^{-1}V_1^T \otimes\ U_2U_2^T)\ \text{vec}(\Delta\mathcal{H}^{(0)}). \tag{A.3}$$

This perturbation is now propagated to the left null space $S_0 = U_2$. From $U_1^T U_2 = 0$ it follows $\Delta U_1^T U_2 + U_1^T \Delta U_2 = 0$, leading to

$$(I_s \otimes U_1^T)\ \mathrm{vec}(\Delta U_2) = -(U_2^T \otimes I_n)\ \mathcal{P}_{t,n}\ \mathrm{vec}(\Delta U_1) \tag{A.4}$$

after vectorization. Considering $U_2^T U_2 = I$ and thus $\Delta(U_2^T U_2) = 0$, it follows $\Delta U_2^T U_2 + U_2^T \Delta U_2 = 0$ and

$$\mathcal{P}_{s,s}(I_s \otimes U_2^T)\,\mathrm{vec}(\Delta U_2) + (I_s \otimes U_2^T)\,\mathrm{vec}(\Delta U_2) = 0. \tag{A.5}$$

From (A.4) and (A.5), a particular solution for $\mathrm{vec}(\Delta U_2)$ follows as

$$\begin{aligned}\mathrm{vec}(\Delta U_2) &= -(I_s \otimes U_1)(U_2^T \otimes I_n)\ \mathcal{P}_{t,n}\ \mathrm{vec}(\Delta U_1) \\ &= -\mathcal{P}_{s,t}(U_1 \otimes U_2^T)\ \mathrm{vec}(\Delta U_1),\end{aligned} \tag{A.6}$$

using properties of the permutation matrix $\mathcal{P}$ [51]. Since $S_0 = U_2$, and substituting (A.3) into (A.6) finally leads to

$$\mathrm{vec}(\Delta S_0) = \mathcal{J}_{S_0,\mathcal{H}^{(0)}}\mathrm{vec}(\Delta \mathcal{H}^{(0)})$$

where $\mathcal{J}_{S_0,\mathcal{H}^{(0)}} = -\mathcal{P}_{s,t}(U_1 D_1^{-1} V_1^T \otimes S_0^T)$. Then, in (A.2) it holds $\mathcal{J}_{\tilde{\zeta},S_0}\,\mathrm{vec}(\Delta S_0) = \mathcal{J}_{\tilde{\zeta},\mathcal{H}^{(0)}}\mathrm{vec}(\Delta \mathcal{H}^{(0)})$, where

$$\begin{aligned}\mathcal{J}_{\tilde{\zeta},\mathcal{H}^{(0)}} &= \mathcal{J}_{\tilde{\zeta},S_0}\mathcal{J}_{S_0,\mathcal{H}^{(0)}} \\ &= (\mathcal{H}^T \otimes I_s)\ \mathcal{P}_{t,s}(-\mathcal{P}_{s,t})(U_1 D_1^{-1} V_1^T \otimes S_0^T) \\ &= -\mathcal{H}^T U_1 D_1^{-1} V_1^T \otimes S_0^T \\ &= -V_1 V_1^T \otimes S_0^T\end{aligned}$$

since the asymptotic covariance can be evaluated in the reference state at $\mathcal{H} = \mathcal{H}^{(0)}$. Then it follows from (A.2) the desired sensitivity $\mathcal{J}_g$ in (A.1)

$$\mathcal{J}_g = \begin{bmatrix}\mathcal{J}_{\tilde{\zeta},\mathcal{H}^{(0)}} & \mathcal{J}_{\tilde{\zeta},\mathcal{H}}\end{bmatrix} = \begin{bmatrix}-V_1 V_1^T \otimes S_0^T & I_{qr} \otimes S_0^T\end{bmatrix}\ . \tag{A.7}$$

References

[1] C. Farrar, K. Worden, An introduction to structural health monitoring, Philosophical Transactions of the Royal Society A: Mathematical, Physical and Engineering Sciences 365 (1851) (2007) 303–315.

[2] A. Rytter, Vibrational based inspection of civil engineering structures, Ph.D. thesis, Aalborg University, Aalborg, Denmark (1993).

[3] K. Worden, C. Farrar, G. Manson, G. Park, The fundamental axioms of structural health monitoring, Proceedings of the Royal Society A: Mathematical, Physical and Engineering Science 463 (2082) (2007) 1639–1664.

[4] M. Basseville, M. Abdelghani, A. Benveniste, Subspace-based fault detection algorithms for vibration monitoring, Automatica 36 (1) (2000) 101–109.

[5] M. Döhler, L. Mevel, F. Hille, Subspace-based damage detection under changes in the ambient excitation statistics, Mechanical Systems and Signal Processing 45 (1) (2014) 207–224.

[6] S. W. Doebling, C. R. Farrar, M. B. Prime, A summary review of vibration-based damage identification methods, The Shock and Vibration Digest 30 (2) (1998) 91–105.

[7] E. Carden, P. Fanning, Vibration based condition monitoring: a review, Structural Health Monitoring 3 (4) (2004) 355–377.

[8] O. Avci, O. Abdeljaber, S. Kiranyaz, M. Hussein, M. Gabbouj, D. J. Inman, A review of vibration-based damage detection in civil structures: From traditional methods to machine learning and deep learning applications, Mechanical Systems and Signal Processing 147 (2021) 107077.

[9] L. Ramos, L. Marques, P. Lourenço, G. De Roeck, A. Campos-Costa, J. Roque, Monitoring historical masonry structures with operational modal analysis: Two case studies, Mechanical Systems and Signal Processing 24 (5) (2010) 1291–1305.

[10] G. Oliveira, F. Magalhães, Á. Cunha, E. Caetano, Vibration-based damage detection in a wind turbine using 1 year of data, Structural Control and Health Monitoring 25 (11) (2018) e2238.

[11] C. Rainieri, G. Fabbrocino, Automated output-only dynamic identification of civil engineering structures, Mechanical Systems and Signal Processing 24 (3) (2010) 678 – 695.

[12] E. P. Carden, J. M. Brownjohn, ARMA modelled time-series classification for structural health monitoring of civil infrastructure, Mechanical Systems and Signal Processing 22 (2) (2008) 295 – 314.

[13] H. Sohn, J. Czarnecki, C. Farrar, Structural health monitoring using statistical process control, Journal of Structural Engineering 126.

[14] D. Bernal, Kalman filter damage detection in the presence of changing process and measurement noise, Mechanical Systems and Signal Processing 39 (1-2) (2013) 361–371.

[15] A.-M. Yan, P. D. Boe, J.-C. Golinval, Structural damage diagnosis by Kalman model based on stochastic subspace identification, Structural Health Monitoring 3 (2) (2004) 103–119.

[16] M. D. Ulriksen, D. Tcherniak, P. H. Kirkegaard, L. Damkilde, Operational modal analysis and wavelet transformation for damage identification in wind turbine blades, Structural Health Monitoring 15 (4) (2016) 381–388.

[17] Z. Tang, Z. Chen, Y. Bao, H. Li, Convolutional neural network-based data anomaly detection method using multiple information for structural health monitoring, Structural Control and Health Monitoring 26 (1) (2019) e2296.

[18] S. D. Fassois, J. S. Sakellariou, Statistical time series methods for SHM, Encyclopedia of structural health monitoring.

[19] F. Kopsaftopoulos, S. Fassois, Vibration based health monitoring for a lightweight truss structure: Experimental assessment of several statistical time series methods, Mechanical Systems and Signal Processing 24 (7) (2010) 1977 – 1997, special Issue: ISMA 2010.

[20] K. Worden, G. Manson, N. Fieller, Damage detection using outlier analysis, Journal of Sound and Vibration 229 (3) (2000) 647–667.

[21] N. Dervilis, I. Antoniadou, R. Barthorpe, E. Cross, K. Worden, Robust methods for outlier detection and regression for SHM applications, International Journal of Sustainable Materials and Structural Systems 2 (1-2) (2015) 3–26.

[22] L. Balsamo, R. Betti, Data-based structural health monitoring using small training data sets, Structural Control and Health Monitoring 22 (10) (2015) 1240–1264.

[23] K. Krishnan Nair, A. Kiremidjian, Time series based structural damage detection algorithm using Gaussian mixtures modeling, Journal of Dynamic Systems Measurement and Control 129 (3) (2007) 285–293.

[24] M. L. Fugate, H. Sohn, C. R. Farrar, Vibration-based damage detection using statistical process control, Mechanical systems and signal processing 15 (4) (2001) 707–721.

[25] J. Kullaa, Damage detection of the Z24 bridge using control charts, Mechanical Systems and Signal Processing 17 (1) (2003) 163 – 170.

[26] L. F. F. Miguel, L. F. F. Miguel, J. Kaminski, J. D. Riera, Damage detection under ambient vibration by harmony search

algorithm, Expert Systems with Applications 39 (10) (2012) 9704 – 9714.

[27] M. Chandrashekhar, R. Ganguli, Uncertainty handling in structural damage detection using fuzzy logic and probabilistic simulation, Mechanical Systems and Signal Processing 23 (2) (2009) 384 – 404.

[28] E. Simoen, G. De Roeck, G. Lombaert, Dealing with uncertainty in model updating for damage assessment: A review, Mechanical Systems and Signal Processing 56-57 (2015) 123 – 149.

[29] T. Kernicky, M. Whelan, E. Al-Shaer, Vibration-based damage detection with uncertainty quantification by structural identification using nonlinear constraint satisfaction with interval arithmetic, Structural Health Monitoring 18 (5-6) (2019) 1569–1589.

[30] Z. Mao, Uncertainty Quantification in Vibration-Based Structural Health Monitoring for Enhanced Decision-Making Capability, Ph.D. thesis, University of California, San Diego (Jan. 2012).

[31] E. P. Carden, A. Mita, Challenges in developing confidence intervals on modal parameters estimated for large civil infrastructure with stochastic subspace identification, Structural Control and Health Monitoring 18 (1) (2011) 53–78.

[32] M. Döhler, L. Mevel, Q. Zhang, Fault detection, isolation and quantification from Gaussian residuals with application to structural damage diagnosis, Annual Reviews in Control 42 (2016) 244–256.

[33] A. Benveniste, M. Basseville, G. Moustakides, The asymptotic local approach to change detection and model validation, IEEE Transactions on Automatic Control 32 (7) (1987) 583–592.

[34] M. Döhler, L. Mevel, Subspace-based fault detection robust to changes in the noise covariances, Automatica 49 (9) (2013) 2734–2743.

[35] E. Balmès, M. Basseville, F. Bourquin, L. Mevel, H. Nasser, F. Treyssède, Merging sensor data from multiple temperature scenarios for vibration-based monitoring of civil structures, Structural Health Monitoring 7 (2) (2008) 129–142.

[36] E. Balmès, M. Basseville, L. Mevel, H. Nasser, Handling the temperature effect in vibration-based monitoring of civil structures: a combined subspace-based and nuisance rejection approach, Control Engineering Practice 17 (1) (2009) 80–87.

[37] E. Viefhues, M. Döhler, F. Hille, L. Mevel, Fault detection for linear parameter varying systems under changes in the process noise covariance, in: Proc. 21st IFAC World Congress, 2020.

[38] E. Balmès, M. Basseville, L. Mevel, H. Nasser, W. Zhou, Statistical model-based damage localization: a combined subspace-based and substructuring approach, Structural Control and Health Monitoring 15 (6) (2008) 857–875.

[39] S. Allahdadian, M. Döhler, C. Ventura, L. Mevel, Towards robust statistical damage localization via model-based sensitivity clustering, Mechanical Systems and Signal Processing 134 (2019) 106341.

[40] M. Döhler, F. Hille, L. Mevel, W. Rücker, Structural health monitoring with statistical methods during progressive damage test of S101 Bridge, Engineering Structures 69 (2014) 183–193.

[41] C. Ventura, P. Andersen, L. Mevel, M. Döhler, Structural health monitoring of the Pitt River Bridge in British Columbia, Canada, Proc. 6th World Conference on Structural Control and Monitoring, Barcelona, Spain, 2014.

[42] J.-N. Juang, Applied system identification, Prentice Hall, Englewood Cliffs, NJ, USA, 1994.

[43] B. Peeters, G. De Roeck, Reference-based stochastic subspace identification for output-only modal analysis, Mechanical Systems and Signal Processing 13 (6) (1999) 855–878.

[44] P. Van Overschee, B. De Moor, Subspace Identification for Linear Systems: Theory, Implementation, Applications, Kluwer, Dordrecht, The Netherlands, 1996.

[45] P. Mellinger, M. Döhler, L. Mevel, Variance estimation of modal parameters from output-only and input/output subspace-based system identification, Journal of Sound and Vibration 379 (2016) 1–27.

[46] L. Mevel, L. Hermans, H. Van der Auweraer, Application of a subspace-based fault detection method to industrial structures, Mechanical Systems and Signal Processing 13 (6) (1999) 823–838.

[47] E. Hannan, Multiple time series, Wiley, New York, 1970.

[48] G. Casella, R. Berger, Statistical inference, Duxbury Press, Pacific Grove, CA, USA, 2002.

[49] A. Mendler, M. Döhler, C. E. Ventura, A reliability-based approach to determine the minimum detectable damage for statistical damage detection, Mechanical Systems and Signal Processing 154 (2021) 107561.

[50] M. Döhler, F. Hille, L. Mevel, Vibration-based monitoring of civil structures with subspace-based damage detection, in: E. Ottaviano, A. Pelliccio, V. Gattulli (Eds.), Mechatronics for Cultural Heritage and Civil Engineering, Springer International Publishing, Cham, 2018, pp. 307–326.

[51] M. Döhler, L. Mevel, Efficient multi-order uncertainty computation for stochastic subspace identification, Mechanical Systems and Signal Processing 38 (2) (2013) 346–366.

[52] J. Liu, X. Liu, X. Ma, First-order perturbation analysis of singular vectors in singular value decomposition, IEEE Transactions on Signal Processing 56 (7) (2008) 3044–3049.